4D printing of polymeric materials for tissue and organ regeneration

Shida Miao [1], Nathan Castro [1,2], Margaret Nowicki [1], Lang Xia [1], Haitao Cui [1], Xuan Zhou [1], Wei Zhu [1], Se-jun Lee [1], Kausik Sarkar [1], Giovanni Vozzi [3], Yasuhiko Tabata [4], John Fisher [5,*], Lijie Grace Zhang [1,6,7,*]

[1] Department of Mechanical and Aerospace Engineering, The George Washington University, Washington DC 20052, USA
[2] Institute of Health and Biomedical Innovation, Queensland University of Technology, Queensland 4059 Australia
[3] Department of Ingegneria dell'Informazione (DII), University of Pisa, Largo Lucio Lazzarino, 256126 Pisa, Italy
[4] Department of Regeneration Science and Engineering, Institute for Frontier Life and Medical Sciences, Kyoto University, 53 Kawara-cho Shogoin, Sakyo-ku, Kyoto 606-8507, Japan
[5] Fischell Department of Bioengineering, University of Maryland, College Park, MD 20742, USA
[6] Department of Biomedical Engineering, The George Washington University, Washington DC 20052, USA
[7] Department of Medicine, The George Washington University, Washington DC 20052, USA

Four dimensional (4D) printing is an emerging technology with great capacity for fabricating complex, stimuli-responsive 3D structures, providing great potential for tissue and organ engineering applications. Although the 4D concept was first highlighted in 2013, extensive research has rapidly developed, along with more-in-depth understanding and assertions regarding the definition of 4D. In this review, we begin by establishing the criteria of 4D printing, followed by an extensive summary of state-of-the-art technological advances in the field. Both transformation-preprogrammed 4D printing and 4D printing of shape memory polymers are intensively surveyed. Afterwards we will explore and discuss the applications of 4D printing in tissue and organ regeneration, such as developing synthetic tissues and implantable scaffolds, as well as future perspectives and conclusions.

Introduction

Four dimensional (4D) printing was first introduced in 2013 and immediately spurred great attention in various research areas including, but not limited to, smart materials and biomedical research [1–3]. Most 4D structures are developed by incorporating shape transformation within material/structural design, which contributes to the 4D definition: 3D printing of objects which can, immediately after printing, self-transform in form or function when exposed to a predetermined stimulus, including osmotic pressure, exposure to heat, current, ultraviolet light, or other energy sources [1,4–7]. Shape memory materials have the inherent capacity to fix a temporary shape and recover their permanent structure under suitable stimuli, which is extremely similar in principle with the 4D dynamic process [8–11]. 3D printing of shape memory materials is reported as novel 4D printing in recent articles; this is becoming a new, and rapidly expanding, research area in 4D printing [12–16].

One argument in this field is whether controlled degradation of 3D printed constructs can be classified as a 4D effect, a claim noted in some articles [13,17]. 3D printing has demonstrated great potential in biomedical fields [18–23]. If biodegradation is included as a tunable mechanism of incorporating a time-dependent effect, 3D printing of timed-release therapeutics and other biodegradable structures fall under 4D printing [18–20]. A point of critique in this argument is that the 3D printed structures noted above completely disappear in the dynamic processes. On the contrary, in shape or functional transformation through the

* Corresponding authors.
E-mail addresses: Fisher, J. (jpfisher@umd.edu), Zhang, L.G. (lgzhang@gwu.edu).

4D process, most of the 3D printed structures remain intact; that is, the 3D fabricated structures are the carrier of the shape or functionality shift as a product of the material properties of the print medium. As such, degradation of 3D printed constructs will not be treated as a 4D effect in this context.

Although the surrounding environments may change significantly during the 4D process, the configuration or function before and after the stimulation should be structurally or functionally stable [12,24]. For example, if a 3D fabricated construct has a primary conformation "A" in air and changes to conformation "B" in water, both conformations should be structurally stable, without external forces to maintain its structure [2]. In the literature, this stable feature is also interpreted as the degree-of-freedom (DOF) should be zero in any state before and after stimulation; herein the DOF refers to the number of independent parameters that define the configuration of a mechanical system [12].

In this review, we will thoroughly summarize the proceedings of 4D printing and its applications in tissue and organ regeneration. We will organize the material based on fabrication approaches and mechanisms. Recent review articles have been published on varying aspects of this field, which are beyond the scope of the current review. The reader is directed to these review articles for further investigation [12,13,17,25–27].

## 4D printing – integration of transforming information in structural design

Bases on the concept of 4D printing, the fabricated structure performs a self-assembly process immediately after 3D printing; this self-assembly is a process in which a pre-existing form dynamically changes to another structure as a consequence of external stimuli. Actually, 3D printing of self-assembly structures existed prior to the definition of 4D printing [28,29]. For example, shape-changing architectures were inkjet printed by patterning light-absorbing ink onto a prestrained polystyrene substrate; the ink acted like hinges to induce an autonomous shape change while they transferred the absorbed heat to the underlying substrate [28]. Additionally, 3D aqueous droplets, with a volume of ~65 pL, were ejected into a lipid containing oil bath and programmed into pre-designed, bilayered networks which swelled or shrank in response to water flow, resulting from osmotic-pressure differences; a variety of shapes were fabricated through the use of droplet networks [29]. 4D printing, however, is catching greater attention, in various research fields, after the definition was coined.

Water sensitive 4D structures, printed with two different materials with different water absorption capacities, came into light with the concept of 4D printing [30]. The water-absorbing material was printed on one side with a rigid waterproof material on the other side. After the printed structure was put into a water bath, the volume of the water-absorbing material increased significantly, up to 150%; in contrast, the waterproof material remained unchanged. The water-stimulated volume difference caused the structure to bend toward the rigid side. The folding halted after reaching the final-state configuration when rigid neighboring elements contacted each other through pre-designed models. Hinges

were designed with this two-layer-material structure where the constructs programmed by material changes could deform into predesigned 3D configurations when submerged in water. As shown in Fig. 1a, a single strand containing both the rigid and active materials transformed into the letters "MIT" when it was placed in water, demonstrating a 1D to 2D shape change [30]. In Fig. 1b, the flat plane on the left is the unfolded surfaces of a six-sided cube; a long strip of active and rigid materials were printed at each of joints. This plane folds automatically into a closed-surface cube when submerged in water, exhibiting a 2D to 3D transformation [30]. Fig. 1c illustrates the structural design of a folding primitive, where the desired folding angle is achieved by adjusting the distances between the small rigid disks that act as stoppers [31].

Besides folding, other transformations such as curling, twisting and linear expansion can also be achieved using highly specific joint designs [31]. Raviv et al. modeled three primitives: a folding primitive, a linear stretching primitive, and a ring stretching primitive [31]. The folding primitive is as described in Fig. 1c. The linear stretching primitive is demonstrated in Fig. 1d; the length and the percent of stretch is controllable by adjusting the ratio of expanding material as shown in red in Fig. 1d. The ring stretching primitive is shown in Fig. 1e where a ring structure is expanded into a bar shape. Different materials are used to fabricate the inner and outer rings. When the structure is put into water, the expanding inner ring will force the structure to transform into a bar shape. By applying different ring sizes in different patterns, complex structures could be designed and realized. As shown in Fig. 1f, a designed grid was deformed into a surface with double curvature when placed in water [31].

With similar layered structural design elements, bio-based wood material was used to 4D print hygroscopically active structures, which is significantly interesting since wood is one of the most common renewable materials [32]. Fused deposition modeling (FDM) printable wood filaments have been developed by combining microwood fibers with suitable 3D printing polymers [32–34]. More interestingly, the extruded wood fibers retain their hygroscopic activity, swelling/shrinking in response to humidity changes, as well as exhibiting anisotropic properties attributable to the shear forces induced upon the material during the printing process [32]. These characteristics allow the 3D printed wood structures to exhibit 4D effects by responding to moisture; various curling or folding deformations have been programmed by designing the pattern and orientation of each layer, the layer height, and the layer interactions [32]. As shown in Fig. 1g, the printed aperture can sense relative humidity, opening at low relative humidity and closing at high relative humidity [32]. In this structure, wood filament was combined with acrylonitrile butadiene styrene (ABS) filament, which acted as a nonresponsive material because of its low water absorption and mild flexibility. The shear stress between the two materials drives the shape transformation. Nylon was also utilized to fabricate multimaterial composites. Interestingly, the nylon remained in the interior of the radius of curvature during the shape transformation while the wood remained outside. When used with ABS, the contrary was noted. Therefore, hygroscopic wood materials can be precisely programmed and manipulated to sense fluctuations in
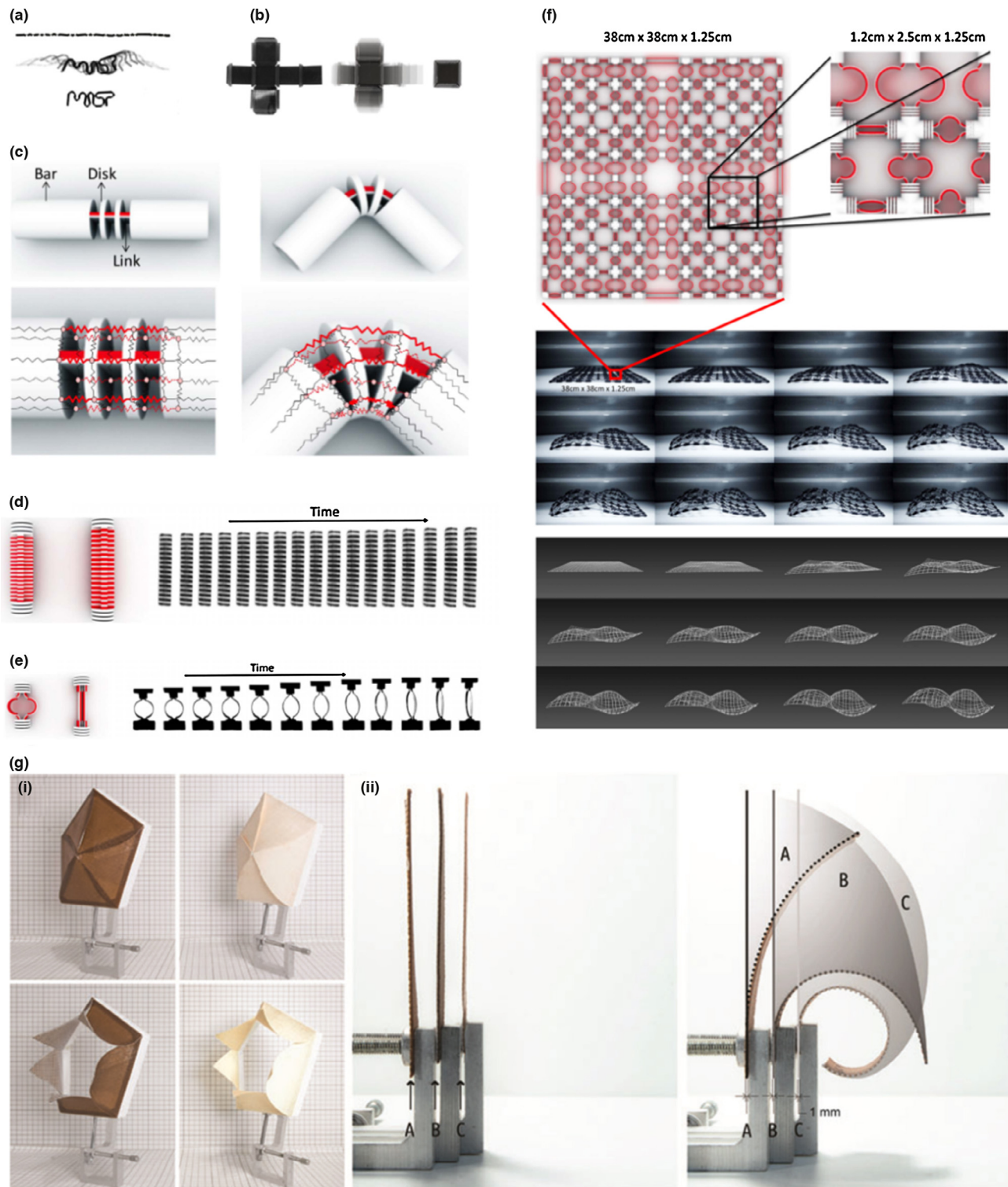
FIGURE 1

(a) A single strand transformed into the letters "MIT. (b) A plane folded automatically into a closed-surface cube. (c) The structure design of the folding primitive and red part is a water-expanding material. (d) A linear stretching primitive. (e) A ring stretching primitive. (f) An example embedding dynamic primitives of stretching and folding on a grid, which accommodates a self-evolving deformation into a complex double curvature surface. (g) (i) The performance of the responsive 3D printed aperture (left) as compared to the veneer-composite system aperture (right) adapting to relative humidity changes: open at low relative humidity (low) and closed at high relative humidity (up); (ii) Three 1-mm-thick test samples (left) programmed to respond with different curvature ranges due to an increase/decrease in relative humidity level (right). Adapted with permission from [30–32].
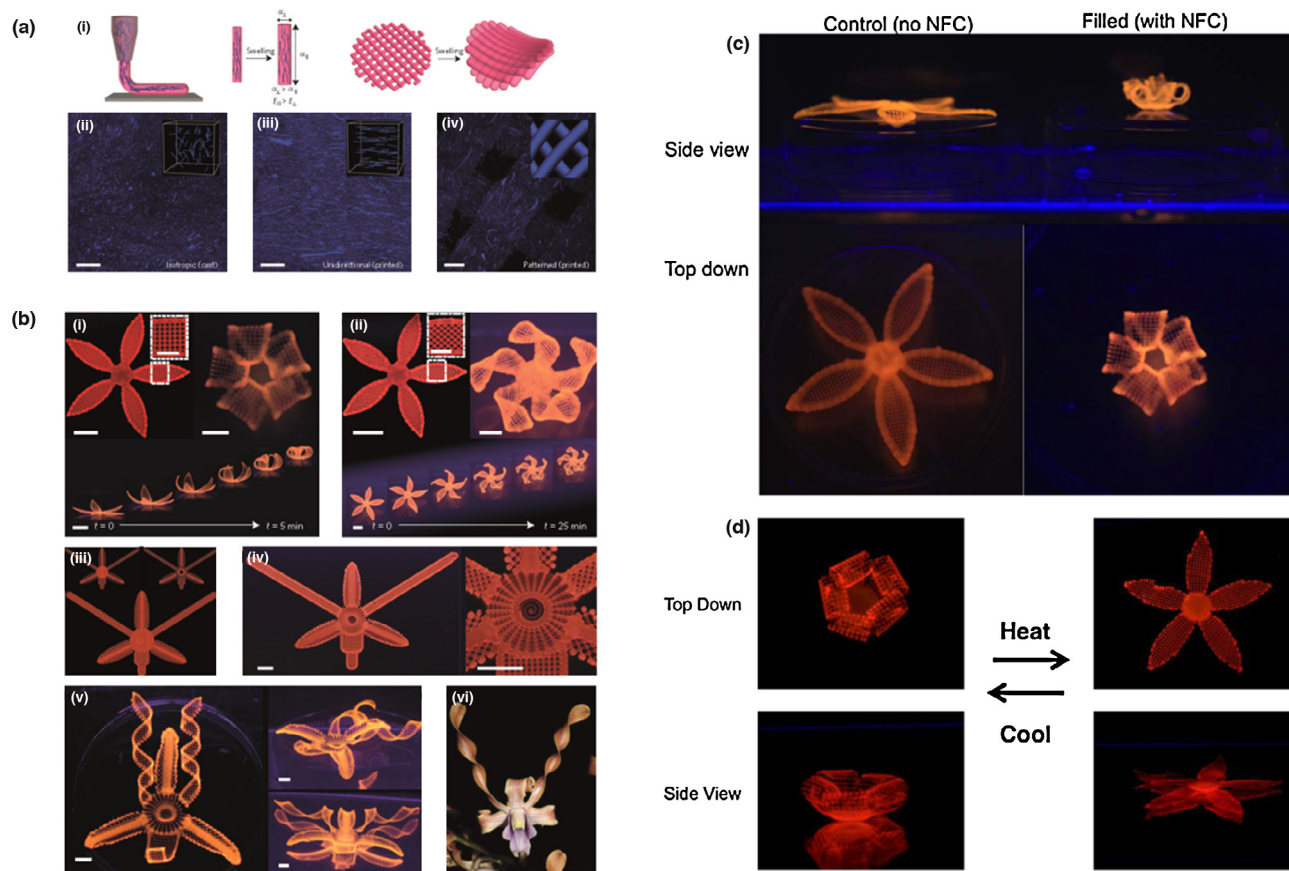
RESEARCH: Review

FIGURE 2

(a) One-step alignment of cellulose fibrils during hydrogel composite ink printing. (i) Schematic illustration of the shear-induced alignment of cellulose fibrils during direct ink writing and subsequent effects on anisotropic stiffness and swelling strain. (ii–iv) Direct imaging of cellulose fibrils (stained blue) in isotropic (cast) (ii), unidirectional (printed) (iii) and patterned (printed) (iv) samples (scale bar, 200 μm). (b) Complex flower morphologies generated by biomimetic 4D printing. (c) Controlled flower architecture composed of hydrogel ink with 0 wt% (left), compared to flower architecture (right) with 0.8 wt% nanofibrillated cellulose (NFC). (d) Thermoreversible shape change of a flower composed of a poly(N-isopropylacrylamide) (PNIPAm) hydrogel matrix with 0.8 wt% NFC. Adapted with permission from [2].

the environment and react through self-transformation by using multimaterial 3D printing technologies and anisotropic material compositions.

Beyond layered structural design, 4D biomimetic printing of complex, shape-changing, natural analogues, such as flowers and leaves which transform after exposure to water, was performed with nano inks [2]. The ink was formulated including synthetic hectorite clay, nanofibrillated cellulose, and N,N-dimethylacrylamide or N-isopropylacrylamide (NIPAM) monomers. As the ink was extruded out of the nozzle during printing, a fraction of the cellulose component was, as observed in extruding wood fibers [32], self-aligned in the hydrogel due to the shear stresses, which resulted in anisotropic swelling of the extruded fiber along the longitudinal direction, shown in Fig. 2a. The core technology of this research varies from other work in that controlling the anisotropic swelling property can precisely predetermine the folding of the bilayered structures upon swelling. Fig. 2b(i) illustrates a closed flower shape when a 90°/0° angle arrangement was printed in the bilayer petal structure; in contrast, convoluted folding was formed when the extruded fibers were printed in a 45°/45° configuration within the petals, as observed in Fig. 2b(ii). Multi shape transformations were also

achieved through this folding mechanism as evidenced by successful mimicking of the orchid Dendrobium (Fig. 2b(iii)–(vi)). Fig. 2c confirms that the cellulose component is critical for the folding behavior because the printed structure without cellulose showed no folding capacity. Fig. 2d further illustrates reversibility of the shape change by replacing N,N-dimethylacrylamide with NIPAM in the ink since the latter is water resistance at high temperature. Compared to single shape change materials, reversible-shape-changing 4D printing may garner greater attention because of the versatility of this feature [35].

One hurdle of current 3D printing techniques is the slow printing speed driven by the additive process [7,30]; interestingly, ultrafast 4D printing was reported, by using digital light exposure on light curable monomers of multi-dimensional responsive polymers including hydrogels and shape memory polymers [14]. Fig. 3a illustrates the printing setup which is capable of controlling light exposure time at each pixel. Using commercial monomers (Fig. 3b), different exposure time resulted in variable degrees of monomer conversion and cross-linking density, which created stresses, converting the 2D shape into a 3D object when the printed structure is immersed in water. As shown in Fig. 3c, a complex theater structure was printed by
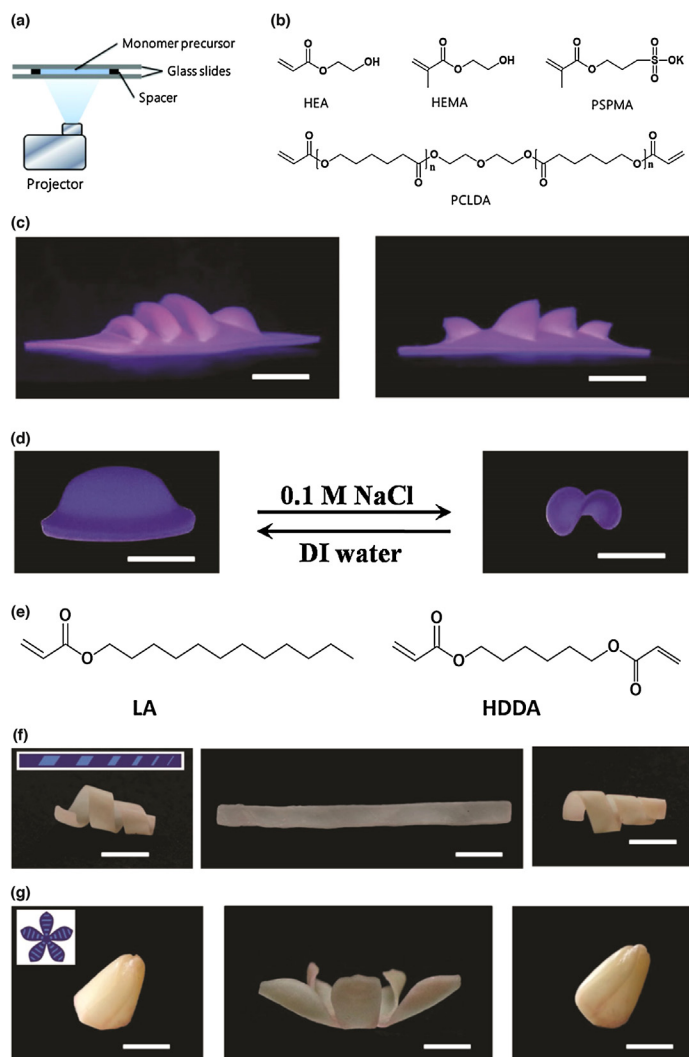
FIGURE 3

(a) Experimental printing setup. (b) Chemical structures of the precursor monomers for the hydrogel system. (c) Photographic images of actual printed 3D theater viewed from two different angles. (d) Printed 4D object with additional active shape changing capability. (e) Chemical structures of the wax-based precursor monomers. (f,g) Shape memory demonstration of a gradient helix and a tulip flower. All scale bars are 1 cm. Adapted with permission from [14].

digital design and highly controlled exposure time. Moreover, the printed structures exhibited reversible shape change by varying the ionic strength of inducing solution (Fig. 3d), which the author claims is the primary actuating mechanism. Per the previously discussed definition of "4D printing", the 3D printing of water actuated materials can be considered 4D printing without the ionic strength response; that is, the transforming information was embedded in the structural design, which induced a conformational change when the structure was immersed in water. Therefore, material response to ionic strength may be classified as a secondary process or an additional dimension beyond 4D. This printing technique has the inherent advantage of flexibility owing to the variation of monomer utilization. By printing wax-based shape memory polymers, the obtained structures can be fixed in a temporary shape which recovers to its permanent shape upon stimulation (Fig. 3e–g). The author claimed that

the shape memory process constitutes 4D printing. As a matter of fact, 3D printing of wax responsive structures can be considered 4D printing, even without shape memory effect, because 3D printing was used to print one conformation which converted to another conformation when placed in melted wax. This process is in full agreement with the definition of 4D printing. The shape memory effect may provide an additional dimension over 4D like the ionic strength did.

An interesting, multimaterial, magnetically-assisted 3D printing (MM-3D printing) platform for composite materials, was controversially reported to enable 5D programmability which might be thus far the first paper to assert this claim [36]. In addition to 3D printing of shape changing materials, local control of the material composition has been deemed an additional dimension, and particle orientation is yet another dimension. The printing setup is shown in Fig. 4a. The two-component mixing and dispensing units, loading with inks of various particle content and resin composition, enable the gradual change in ink position. The external low magnetic field is used to orient the magnetic particles before the extruded ink is consolidated by light. Fig. 4b shows the printed complex's heterogeneous structure with local texture and local composition. This technique is also used to print soft devices which undergo programmed shape change triggered by exposure to ethyl acetate. As shown in Fig. 4c, a printed hollow cuboid fastening system can join two separated tubes when the cuboid is allowed to swell. Fig. 4d shows a printed complex soft key-lock structure which can carry an object much heavier than its own weight. The 3D printing with the additional shape change by soaking with solvent is essentially 4D printing. If adding the previous claim of two additional dimensions, a six dimensional fabrication is achieved. It seems that the authors intended not to name their research as 5D or 6D printing for reasons that are not clear in their presented work. One factor is that particle orientation may not be a "dimension" which cannot perform a dynamic process after printing; similar orientations in other reported works were not treated as an additional dimension [37,38]. Another factor is that 3D printing refers to the three common spatial dimensions which are different from other dimensions, referring to any potential shape or function; in this sense, it may be better to call any 3D printing plus additional dimensions as 4D printing in a broad sense; here 4D extensively refers to any added shape or function integrated into a 3D printed object.

Thus far, 4D printing studies have predominantly focused on biologically-inspired hierarchical morphological changes. Multimaterial printing technology is the preferred technology for both academic and industrial researchers, which in itself is on the fringes of 3D printing [30]. Owing to the distinct properties of different materials, anisotropic properties are readily achievable by depositing multiple materials in various patterns within a composite structure, which drives the 4D dynamic process after external stimuli. Not limited to multi-material printing, 4D printing of single inks is achievable by leveraging the anisotropic properties of the material through aligned printing or by varying the crosslinking density of the fabricated structures [2,14]. In these studies, extrusion based 3D printing technology, for which the ink is forced out of the nozzle, is dominantly applied, while laser-based printing techniques show great potential for hydrogel
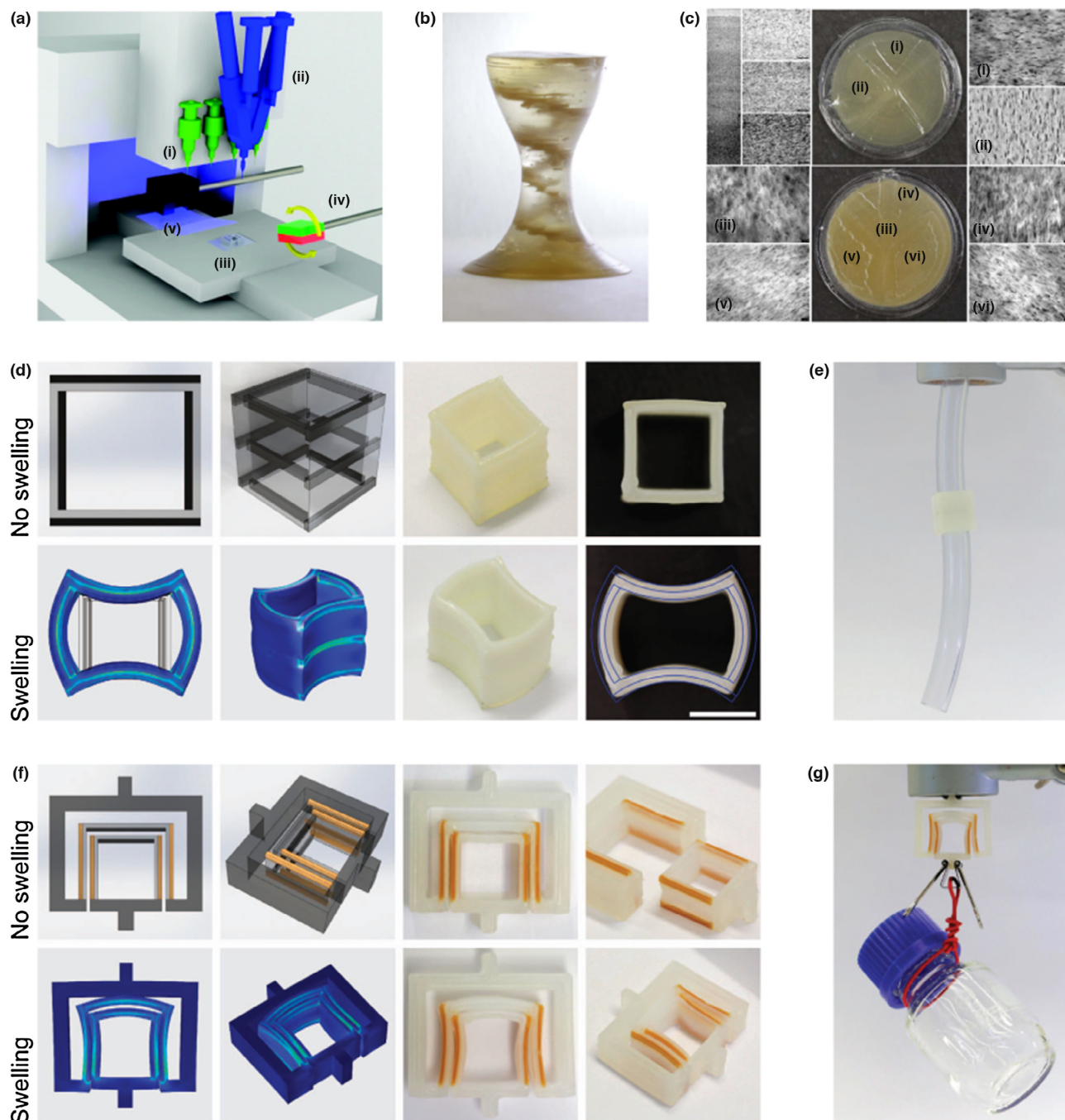
FIGURE 4

(a) Direct ink-writing hardware equipped with multiple dispensers. (b) Actual MM-3D printed object with internal helicoidal staircase. Scale bar, 5 mm. (c) (c; top) Photograph of the top layer of the structure. (c; bottom) Photograph of the bottom layer of the structure. (d) (D; Top) Drawings and actual printed cuboids before the shape change. (d; bottom) Finite element simulations and actual pictures of the cuboids after the shape change. Scale bars, 10 mm. (e) Cuboid-mediated fastening of two tubes achieved through the shape change of the printed object. Scale bar, 20 mm. (f) (f; top) Drawings and actual printed key–lock objects before the shape change. (f; bottom) Finite element simulations and actual pictures of the key–lock structure after the shape change. Scale bars, 15 mm. (g) Mechanical fastening enabled by the shape changing key–lock architecture. Scale bar, 15 mm. In all drawings, light and dark gray colors indicate soft and hard phases, respectively. Adapted with permission from [36].

materials [2,14,30]. Particularly, immersing the 3D printed structures in water or organic solvents is a widely adopted method to trigger a 4D process. Integrating more dynamic changes, beyond 4D, to the printed structures may potentially lead to new and interesting trends in furthering functional materials capable of multiple transformations. Undoubtedly, ongoing 4D printing studies not only build upon a highly active research field but also serve to open pathways for the application of multidisciplinary science and technologies to 3D fabricate novel self-assembled and/or functionally adaptive designs.

4D printing – three dimensional printing of shape memory polymers (SMPs)

Shape memory polymers are attracting greater attention due to stimuli-triggered dynamic processes which exhibit similar characteristics to time-dependent shape changes of 4D printed materials [8,39–41]. Amongst shape memory polymers, heat-activated SMPs are the most widely applied derivatives which demonstrate a broad tunable range of mechanical, thermal, and optical properties [42–44]. Chemical or physical crosslinks in the thermally initiated SMPs are usually utilized to set the permanent shape while a transition temperature (T_{trans}), typically a melting temperature (T_m) or a glass transition temperature (T_g), is used to control the molecular switching segments that fix the temporary shape. As the SMPs are heated above their T_{trans}, the molecular switching segments are "soft" and a deformation can be exerted to set the temporary shape; when the temperature is decreased below the T_{trans}, the molecular switching segments will "freeze" to immobilize the pre-designed temporary shape. The SMPs will recover their permanent shape upon returning to a temperature over T_{trans} since the molecular switching segments are soft again allowing the crosslink networks to revert the structure back to the original shape. In addition to heat-initiated SMPs, a range of different materials have been reported with various shape fixation and shape recovery mechanisms [45,46]. Some modes of actuation include indirect heating. For example, near infrared light or electronic triggers induce a change in temperature, which further drive the shape recovery process [47–49]. With regards to 3D printable inks based on SMPs, direct heat activated SMPs are the dominant variety and will be the primary focus of this discussion.

Shape memory thermoset polymers

Shape memory thermoset polymers can be directly 3D printed with different printing techniques [15,49–51]. For example,

soybean oil epoxidized acrylate was laser printed for the fabrication of biomedical scaffolds [15]. The ink was developed using soybean oil epoxidized acrylate with bis(2,4,6-trimethylbenzoyl)-phenylphosphineoxide as a photopolymerizer. A table top stereolithography (STL) system, based on the existing Solidoodle® 3D printer platform, was utilized to print the scaffolds [52]. The ink was cured by activating the laser and drawing lines at various print speeds.

Similarly, a shape memory tracheal stent was printed with polycaprolactone dimethacrylates using a UV-LED digital light processing (DLP) printer [51]. The wavelength of the UV-LED light source was 405 nm. While STL uses a laser to "draw" the object's layers, DLP projects the entire slice of the object using a digital projector. With DLP techniques, a family of photocurable methacrylate based copolymer networks have been developed and printed via high resolution (up to a few microns) projection microstereolithography (PμSL) (Fig. 5a) [41].

An interesting technique, UV curing of jet sprayed materials, has been utilized to fabricate shape memory structures. The inks are commercially available from the 3D printing company Stratasys (Edina, MN, USA) [53–55]. By combining two model materials VeroWhite® and Tangoblack®, the so-called digital materials were created. Varying compositions of these two materials leads to different thermomechanical properties. By 3D printing hinges using various T_g digital materials, adaptive structures capable of self-expanding and self-shrinking were created [53]. When the structure is subjected to a uniform temperature, temporal sequencing of activation was achieved by the time-dependent behavior of each polymer, which was illustrated via a series of 3D printed structures that respond rapidly to a thermal stimulus and self-fold to specified shapes in a controlled shape-changing sequence (Fig. 5b) [53]. By integrating both material design and the shape memory digital materials, active structures were further developed [55]. Glassy shape memory polymer fibers were directly printed in an elastomeric matrix; after a programmed
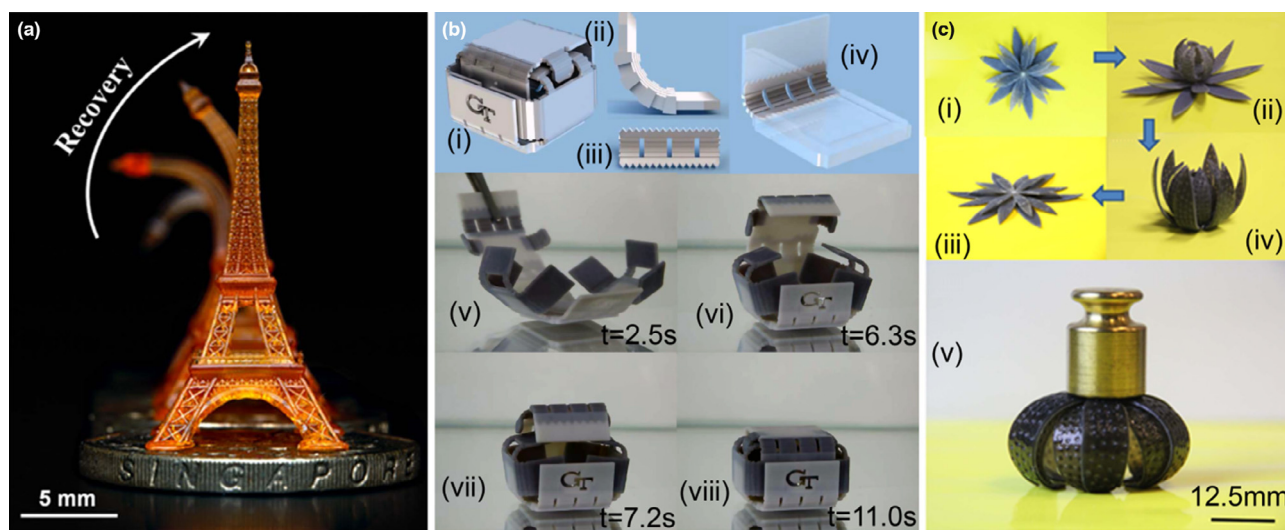

FIGURE 5

3D printing of shape memory thermoset polymers. (a) Shape memory Eiffel tower 3D printed by using high resolution projection microstereolithography (PμSL). (b) (i) 3D printed shape memory folding structure. (ii–iv) The design of the folding box with some details at the hinges. (v-viii) Upon heating, the sheet of temporary shape folds into the box with self-locking mechanism. (c) A self-folding/unfolding flower. (i–iv) The sequence of reversible actuation. (v) The dried configuration is stiff and can carry a load of 25 g. Adapted with permission from [35,41,53].

lamina and laminate architecture and a subsequent thermomechanical training process, the shape memory effect transformed a thin plate into complex three-dimensional configurations including bent, coiled, and twisted strips, folded shapes, and complex contoured shapes with non-uniform, spatially varying curvature [55]. By heating these structures, they recovered their original shape. By 3D printing shape memory polymers and hydrogels in prescribed 3D architectures, a new, reversible, shape-changing component design concept was realized [35]. The swelling of the hydrogel was used to drive the shape change while the temperature-dependent modulus of a shape memory polymer was used to regulate the time of such shape change. Via the controlled interplay between the active materials and the 3D printed architectures, specific shape changing scenarios were achieved (Fig. 5c).

In addition to STL and DLP based printing techniques, extruding techniques are also used to fabricate thermoset shape memory structures. UV cross-linking poly(lactic acid)-based inks were used to print shape memory structures by direct-write printing [50]. Poly lactic acid (PLA), benzophenone and dichloromethane were mixed to create the ink; benzophenone acts as the UV cross-linking agent. All of the fabricating processes proceeded in light resistant conditions at room temperature (25 ± 2 °C). A system consisting of a microdepositing robot was used to direct write the ink. During the printing process, the fast evaporation of dichloromethane was used to harden the 3D structures; shape memory behavior was enhanced by subsequent UV irradiation. Excellent shape memory behavior, which enables multi-dimensional and combinatorial configurations and transformations, was demonstrated. By adding iron oxide, the fabricated structures exhibited fast, remotely actuated, and magnetically guidable properties.

All of the previously described shape memory polymers are cross-linked thermosets which are insoluble and do not flow at high temperature, making them difficult to process [51]. In this regard, resin-based 3D printers (STL or DLP) are preferred for fabrication; liquid monomers or oligomers are placed in a resin bath and photopolymerization is performed layer by layer [15]. As a matter of fact, many thermoset polymers are obtained through a thermal curing process, but most of these types of thermosets are unprintable [56–64].

One solution to use currently unprintable thermoset polymers to construct 3D structures is using sacrificial materials. A mold structure can be 3D printed with sacrificial materials, such as poly lactic acid (PLA) and polyvinyl alcohol (PVA). The monomers for synthesizing the thermoset polymers can then be poured into the mold. After a curing process, the desired scaffolds can be obtained by removing the sacrificial mold material; the mold is leached and the crosslinked thermoset is left. For example, biomimetic gradient tissue scaffolds with highly biocompatible naturally derived smart polymers were fabricated [65]. A series of novel shape memory polymers with excellent biocompatibility and tunable shape changing effects were synthesized and cured in the presence of 3D printed sacrificial PLA molds, which were subsequently dissolved to create controllable, graded porosity within the scaffold. The smart polymers display finely tunable recovery speed and exhibit greater than 92% shape fixing at −18 °C or 0 °C and full shape recovery at physiological temperature. A

graded microporous structure was fabricated, which mimics the non-uniform distribution of porosity found within natural tissues. The finely controlled structure illustrates the feasibility of this strategy for precisely fabricating complex structures. Another advantage of this approach is that this mold-guided technique provides different pore morphologies, facilitating physiologically appropriate, biomimtetic conditions [65].

Shape memory thermoplastic polymers
Thermoplastic polymers are readily used as printing inks [66–73]. FDM printing of a thermoplastic shape memory polyurethane elastomer was reported by Yang et al. [74]. This polymer, DiAPLEX MM-4520, has a degree of crystallinity of 3–50 wt% and is commercial available in pellets from SMP Technologies, Inc [75]. FDM compatible filaments are easily obtained by bulk material extrusion, including shape memory polymer filaments. To guarantee the filament's quality for 3D printing, process parameters for fabricating FDM filaments were first optimized. During 3D printing, nozzle temperature, scanning speed, and part cooling are carefully controlled; this is essential for achieving high quality structures. Different samples with complicated three-dimensional shapes were readily printed and showed good shape memory effects [74].

Besides pure polymers, shape memory PLA/15wt% hydroxyapatite (HA) porous composite scaffolds were fabricated by FDM [76]. Physical entanglement of long PLA chains was used to set the permanent shape. The polymeric chains between the entanglements can be stretched during deformation and used to fix a temporary shape. HA is one of the most common bioactive components to increase osseointegration, having great application toward the repair of bone defects. The addition of HA increases the modulus of the composites and secondarily contributes to the maintenance of the permanent shape. During compression-heating-compression cycles of the 3D printed shape memory scaffolds, the HA particles were found to inhibit the growth of cracks. Shape memory effect, which refers to 98% shape recovery triggered by heating, is assumed to have a self-healing function by narrowing and preventing crack propagation.

Moreover, thermoplastic amphiphilic tri-block copolymers poly(D,L-lactic acid-co-ethylene glycol-co-D,L-lactic acid) (PELA) (Mw = 120 kDa) and HA-PELA composites were also used to fabricate scaffolds [77]. In these amphiphilic polymers, phase separation between the hydrophilic and hydrophobic blocks is responsible for the shape memory behavior [78]. Generally, the phase having a higher thermal transition acts as the physical crosslinks or hard segments, while the lower thermal transition phase acts as the switching phase or soft segments [45]. Results showed that these materials can be deformed and fixed into temporary shapes at room temperature with rapid shape recovery (<3 s) observed at 50 °C. Large deformations can be efficiently achieved (fixing ratio >99%) at −20 °C. With higher HA contents, shape recovery speeds became slower, but high shape recovery (>90%) was achieved upon equilibration for 10 min at 50 °C with up to 20 wt% HA contents in composites; permanent shapes can be recovered at 50 °C. In view of the thermoplastic feature of the copolymer, it was printed with a commercial FDM 3D printer into 3D macroporous scaffolds with similar shape memory properties.

Compared to thermoset polymers, thermoplastic polymers are capable of 3D printing with FDM technology which is cost effective and efficient. However, the different layers of the printed scaffolds were combined by adhesion of the melt processed thermoplastic polymer strands, which significantly affects the mechanical properties of the scaffolds and limits the toughness in 3D printed shape memory polymers. An interesting approach was reported to improve interlayer adhesion and strengthen the printed scaffolds by exposing 3D printed copolymer blends to ionizing radiation [79]. A series of polymers blended with specific radiation sensitizers, such as trimethylolpropane triacrylate and triallyisocyanurate, were prepared and irradiated by gamma rays. Results showed that triallyisocyanurate can effectively crosslink the polymer, and the crosslinks prominently enhance the thermomechanical properties and solvent resistance of the 3D printed polymers when the polymers were irradiated at temperatures near the T_g of the shape memory system. Post-printing crosslinking makes the thermoplastic scaffolds possess partial characteristics of thermoset scaffolds without compromising the FDM printing process; this enables a new method for developing inexpensive 3D printable parts with robust thermomechanical properties.

Novel processes and materials with great potential for 4D printing

In section "4D printing – integration of transforming information in structural design", water-sensitive, humidity-sensitive, thermo-responsive and organic solvent sensitive materials are discussed and highlighted for dynamic 4D processes. Besides these notable functional materials, a myriad of stimuli-responsive systems and novel processes also show great potential for 4D printing.

Thermally-induced novel process

The internal strain/stress during FDM 3D printing has been used to induce patterned transformation(s) [80]. During FDM printing, PLA filaments were maintained in a high temperature furnace and then extruded through a nozzle. Due to the temperature difference within the printing chamber compared to the heating furnace, the extruded material gradually cools and solidifies thereby bonding to the printing platform and previously deposited materials. The internal stress/strain of the material increases during the printing process due to temperature differences and the traction force induced by the feeder motor. At temperatures below the T_g of the material, the internal stress/strain can be stored for an extended period of time. Release of the internal stress/strain is achieved by heating the printed architecture above the T_g which triggers shrinkage, or pattern transformation. Fig. 6a illustrates the transforming process from a ring structure into quadrangles [80]. The shrinkage of printed structures at high temperature is an unwanted effect of FDM, but predesigned structures can be achieved by applying this internal stress/strain to drive a controlled dynamic process.

Multi-layer membrane structures of various materials within each layer can generate a heat-stimulated dynamic process, owing to mismatching coefficients of thermal expansion (CTE)
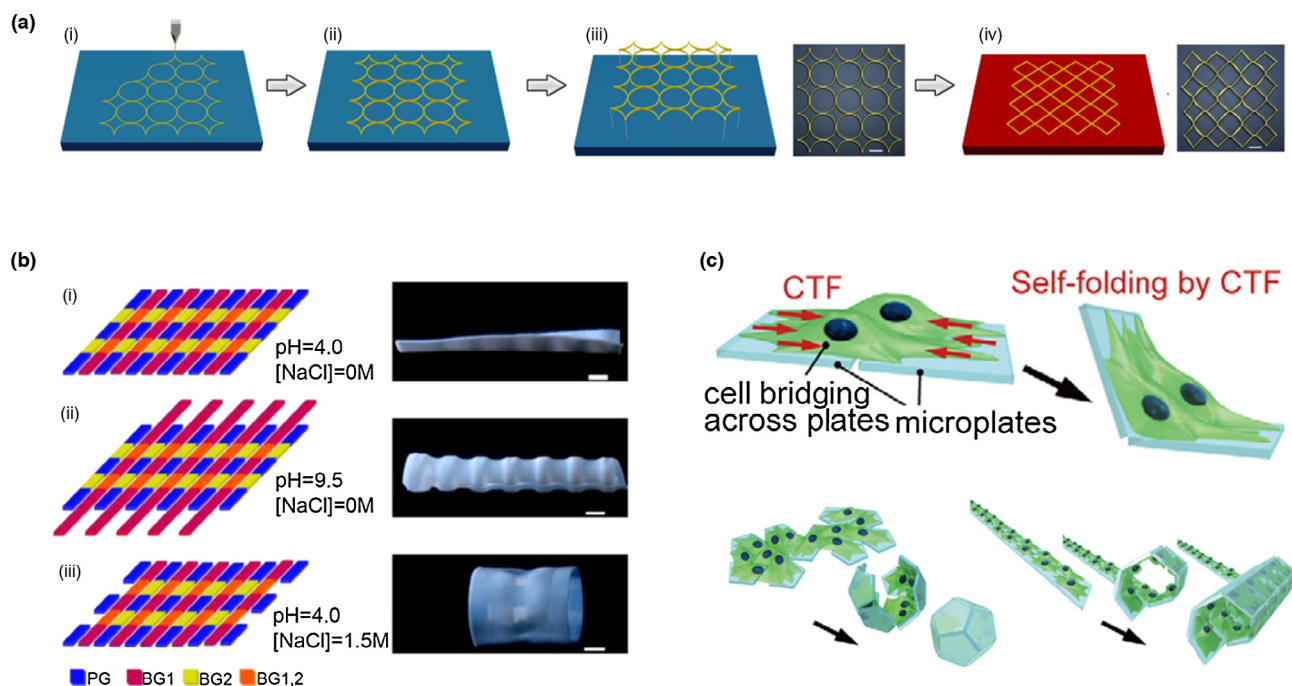

FIGURE 6

Novel processes and materials with great potential for 4D printing. (a) Schematic of 3D printing process and the corresponding deformation of printed polymer described by a viscoelastic model. (i) The fused polymer is extruded from the nozzle and a constant strain is formed due to the moving of nozzle; (ii) The printed polymer cools, solidifies, and bonds with platform or neighboring material and internal strain is generated during the process; (iii) Removing the printed polymer from the platform; (iv) Internal strain stored in the polymer is released when reheated above its glass transition temperature. Scale bar is 12 mm. (b) Multiple shape transformations of the composite gel sheets. The scale bars are 0.5 cm. (c) Schematic image of the cell origami: the cells are cultured on micro-fabricated parylene microplates which are self-folded by CTF. Adapted with permission from [24,80,95].

between materials [81]. Flat PLA strips were printed on a fixed paper sheet; the composite sheet was then cut into a shape with six petals which was then put on a heating plate, at 105 °C, with the PLA layer facing upwards; the center of the composite sheet raised at the beginning and fell gradually to flatten as the temperature increased and reached equilibrium [81]. Interestingly, the planar composite sheet transformed into a flower-like 3D structure when it was cooled down, with the curvature of PLA inside and paper sheet outside; when reheated, the flower structure returned to its original planar shape [81].

Light-triggered dynamic process

In addition to heat, light can reversibly induce conformation changes of certain materials [82–84]. A smart box with reduced graphene oxide-carbon nano tubes/polydimethylsiloxane actuators as the hinges can be unfold by exposing simulated sunlight irradiation and fold when the light is removed [83]. A laminated structure was constructed for achieving photo-induced deformation [85]. The laminated structure consisted of three bonded layers. A stretchable elastomeric sheet was printed between two light active polymer layers. When one side of the light active polymer layer was radiated to be optically relaxed, the stress in the middle elastomeric sheet was released, triggering bending deformation.

Self-healing hydrogel materials

Self-healing, synthesized, polymeric materials have been developed for fabricating three-dimensional biomimetic tissues such as skin [86]. In particular, hydrogel materials exhibit a 3D network structure and excellent water-retention abilities, providing conditions similar to those of the extracellular matrix [86]. Thus, soft hydrogels are assumed ideal materials for use as scaffolds in tissue engineering applications [87–89]. Hydrogels have been utilized in many commercialized products including wound dressings, contact lenses, and personal hygiene products [90]. Hydrogels loaded with biologically active compounds, such as drugs and antibodies, are a highly active research area, and hydrogels also show great promise for the development of artificial implants [91–93]. More importantly, self-healing hydrogels can intrinsically and automatically heal damaged tissue and restore normalcy; this shows a similar dynamic process as 4D printing and greatly motivates the exploration of self-healing hydrogels in the field of tissue and organ regeneration [86]. The self-healing mechanism occurs as the structure of the hydrogel, along with electrostatic attraction forces, drive new bond formation through reconstructive covalent dangling side chains or non-covalent hydrogen bonding [86]. Although 4D printing of self-healing hydrogel materials is not reported thus far, a myriad of hydrogel materials with potential for 3D/4D printing are predicted and reviewed [86].

Integrated multiple transformations triggered by different stimuli

As "single" shape changing structures have catalyzed the smart material realm, studies on the development of materials and structures that can be configured and reconfigured multiple times into different shapes with the use of different stimuli are covertly revolutionizing related fields [24,94]. Multiple shape transforma-

tions, each triggered by a particular external stimulus, were achieved with a planar hydrogel sheet integrated with multiple small-scale polymer components with distinct compositions [24]. Internal stresses within the composite hydrogel sheet are created as the structural components undergo differential swelling or shrinkage in response to different stimuli (i.e. temperature, pH, ionic strength, or CO_2 supply (Fig. 6b)[24]. The complicated microenvironments in the human body are physiological analogues to this concept and contain multiple regulatory processes, such as neuroregulation, self-regulation, and humoral regulation. Therefore, multi responsive materials may provide better conditions for biomedical applications. Discovering novel multi responsive materials, or evaluating and transforming the printability and biocompatibility of existing multi responsive materials, may become an exciting research trend.

Other functional aspects for 4D printing

In addition to material design and smart materials, the traction force of living cells has been shown to possess the ability of driving various pattern formations [95,96]. As shown in Fig. 6c, cells were seeded across two microplates which were then attached to glass; when the microplates were detached from the glass, the cell traction forces folded the microplates [95]. By using multiple microplates and properly designing the geometrical patterns, various cell-laden microstructures were obtained.

4D printing should not be solely viewed in the veil of shape changes, but rather should include all functional changes. Thus far, little work has been conducted in this area. Avenues to explore may include materials which undergo color change when triggered by specific wavelengths of light [17,97]. Due to the constraints of the definition of "4D printing", this may raise controversial discussion points. The simple addition of color changing materials in 3D printing inks can create light-responsive, color-transforming constructs, but treating this transformation as an additional dimension, may be a stretch and present numerous questions. The breadth and depth of related studies is believed to provide more insights about 4D printing.

Application of 4D printing in tissue and organ regeneration

3D printing has demonstrated its great potential capacity for engineering functional tissues or organs to heal or replace abnormal and necrotic tissues/organs, providing a promising solution to severe tissue/organ shortages [72,98]. 3D printing is evolving into an unparalleled biomanufacturing technology [67,71,99–107]. Based on all the advanced characteristics of 3D printing, 4D printing incorporates a time-dependent dynamic process in the fabrication design, which is believed to further revolutionize current tissue/organ fabricating platforms.

Synthetic tissues, which have the ability to fold and be controlled externally by light, were fabricated by printing structures containing hundreds or thousands of communicating aqueous droplets arranged in programmed patterns [29,108]. First a piezo-based 3D printer capable of printing thousands of aqueous droplets (∼50 pL) in patterned 3D assemblies was constructed (Fig. 7a). The printed droplet networks were generated inside oil drops in an aqueous environment, thus the final structure is
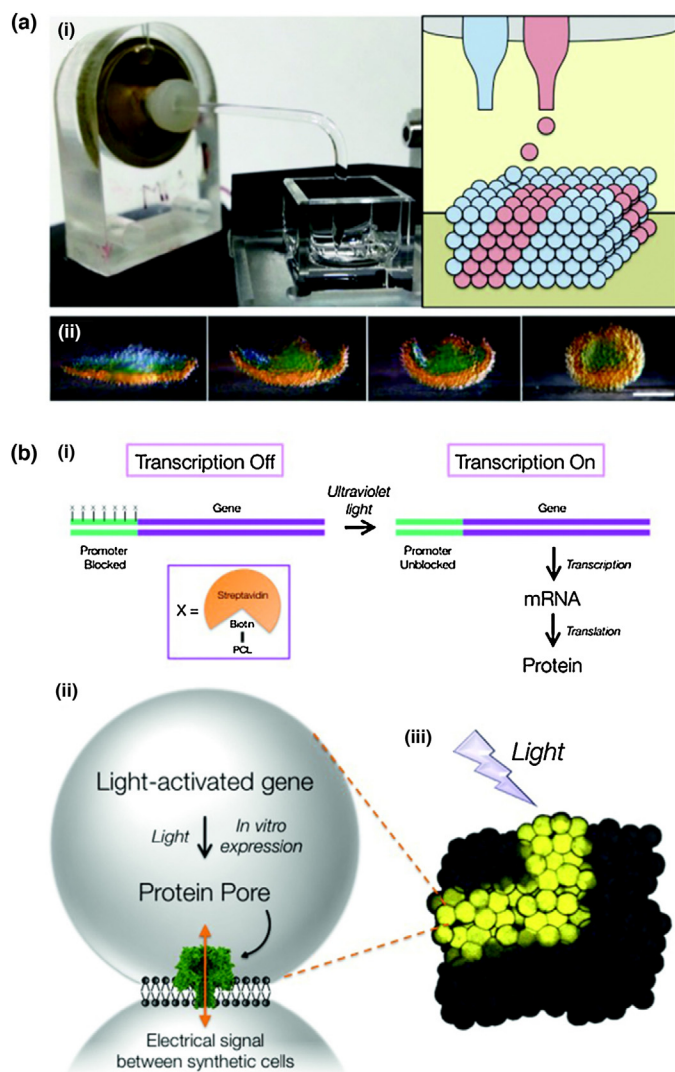
FIGURE 7

Application of 4D printing in synthetic tissues. (a) (i) The 3D droplet printer. (ii) A printed 4-petal structure folded into a hollow sphere. Scale bar, 200 μm. (b) Light-activated synthetic tissues. (i) The LA-DNA carries the small molecule biotin attached through a photocleavable linker (PCL) at several sites on the promoter region of a gene of interest. Biotin binds strongly to the large protein streptavidin, which blocks transcription of the gene by RNA polymerase. Low energy ultraviolet light cleaves the PCL groups, removing the steric block. The DNA can then be transcribed into messenger RNA and translated to protein. (ii) A light-activated gene, encoding a protein pore, is expressed inside synthetic cells, by using an *in vitro* expression system. The resulting protein pores form holes in the lipid membrane between the synthetic cells, allowing electrical communication. (iii) Synthetic cells can be printed into patterned synthetic tissues, which exhibit directional signaling through defined pathways, shown here by the expression of a fluorescent protein. Adapted with permission from [29,108–110].

encased in a lipid bilayer through which communication with the external environment can be mediated using membrane proteins [29,109]. These structures can perform dynamic shape change processes. Layers of droplets with different internal osmolarities were printed into a 4-petal structure, which folded into a hollow sphere when water flowed across the bilayers (Fig. 7a). These structures, with multiple communicating compartments and dynamic shape changing capabilities, are

rendered more analogous to living organisms. Furthermore, these structures could be enhanced to resemble living cells by adding the ability to synthesize protein from encapsulated DNA with an *in vitro* expression system which is controllable by external light [110]. Fig. 7b shows the light-controlling expression system. Biotin is attached at several sites on the promoter region of the gene of interest. Streptavidin, bonded strongly with biotin, was used as a steric blocker of the promoter sequence, thereby preventing transcription of the DNA by RNA polymerase. Photocleavable linkers were inserted between the promoter and the biotins. Thus, the expression system existed in off-state at first; after removal of the block with low energy ultraviolet light, transcription followed by translation of the messenger RNA into protein. Optimizing the number of biotins and their sites of attachment produced the tightly regulated, light activated DNA (LA-DNA) promoter; combining the stabilized aqueous droplet networks with the LA-DNA made light-activated synthetic tissues. By using the expression system under the control of the LA-DNA promoter, α-hemolysin (αHL) pore was created within the synthetic cells (Fig. 7b). The synthetic tissue has no function following 3D printing; αHL was synthesized after irradiation, forming pores in the droplet interface bilayer through which an electrical current could pass. Extended 3D pathways of cells producing αHL were generated within synthetic tissues by patterning the synthetic cells that contained LA-DNA, or using guided irradiation. This resulted in light-activated directional electrical communication realized with external electrodes. These synthetic tissues indicate great potential for use in drug delivery and tissue replacement surgeries. With the multi-compartment nature of these materials, release of binary or ternary agents is possible; components (e.g. an enzyme and a substrate) in the agents are combined at a desired site to generate potent effectors. Synthetic tissues might also be used to replace damaged tissues, especially for providing a provisional electrical connection after nerve damage. Additionally, questions of immunogenicity and uncontrolled proliferation may be lessened with synthetic tissues when compared to therapies based on living cells.

3D fabricated scaffolds can also capitalize on natural characteristics of tissues and organs, thereafter contributing to the restoration of their original functions. 3D printing of shape changing materials combines the merits of additive manufacturing and smart materials, which is promising for the advancement of personalized medical devices. Particularly the shape memory effect of the fabricated scaffolds allows for their autonomous deployment in otherwise inaccessible places. For example, a shape memory tracheal stent was fabricated based on anatomical data; methacrylated polycaprolactone precursor, with a molecular weight of 10,000 g mol^{-1}, was used as the bioink [51]. The printed stent can be deformed into its temporary shape, inserted in the body and then deployed back into its permanent shape with a local increase in temperature; this classifies the scaffold as a minimally invasive medical device.

Development of smart and highly biocompatible materials for 4D printing is becoming an active research area. Scaffolds capable of supporting the growth of multipotent human bone marrow mesenchymal stem cells (hMSCs) were 3D STL printed with soybean oil epoxidized acrylate [15]. Laser frequency and
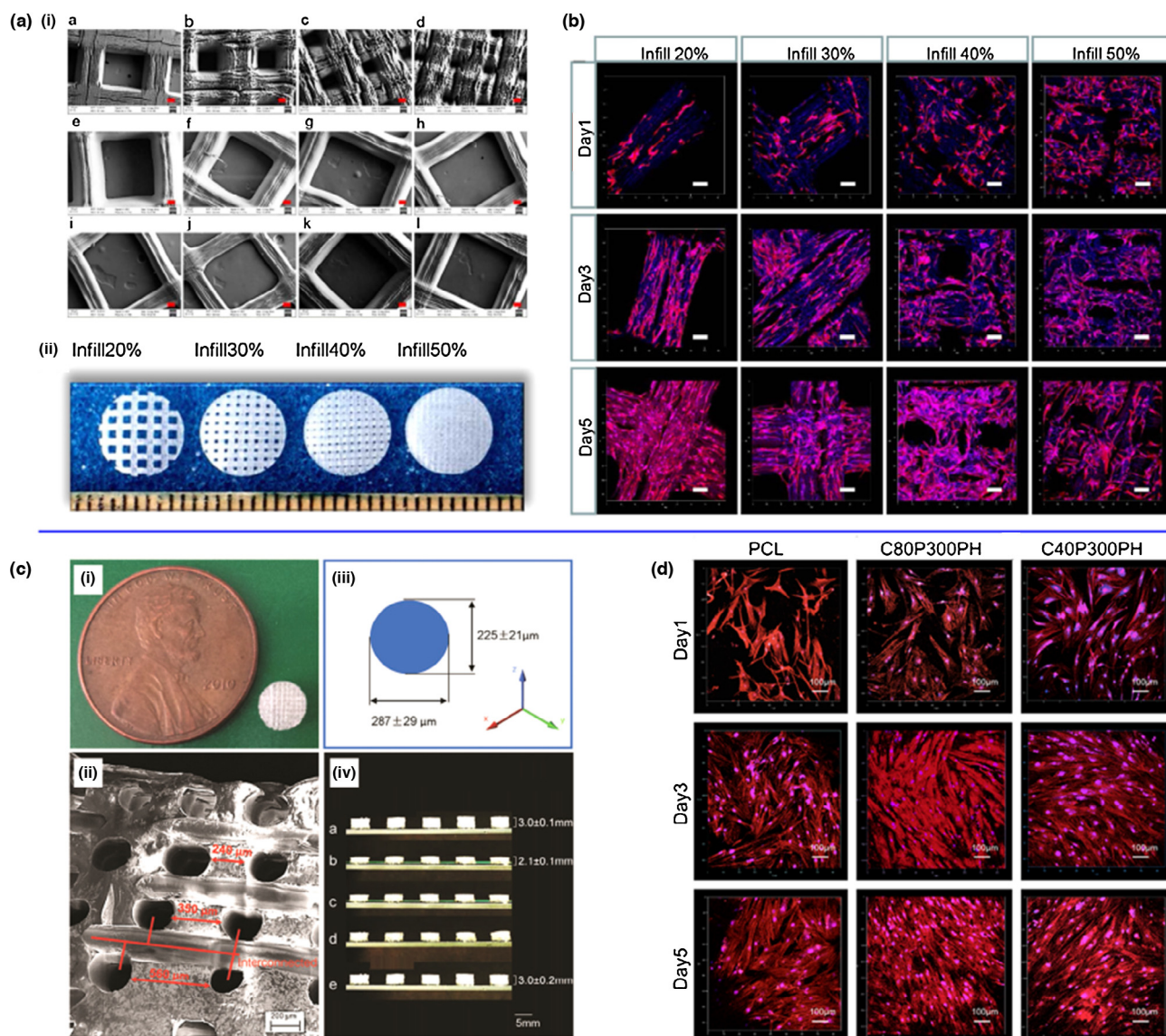
FIGURE 8

Shape memory biomedical scaffolds. (a) (i) SEM images of printed scaffolds, red scale bar 100 μm. (ii) The photos are of the printed scaffolds. (b) Confocal images of hMSCs spreading on printed scaffolds. Scale bars are 100 μm. (c) The fabricated scaffold. (i) A 5-mm-diameter and 3-mm thickness scaffold compared to a penny. (ii) The SEM image of the pore distribution in the scaffold. (iii) Varied pore diameters in different directions. (iv) The potential for minimally invasive application. (d) Confocal microscopy images of hMSC growth and spreading morphology when compared with PCL control after 1-, 3-, and 5-day culture. The color red represents cell cytoskeleton and the color blue represents cell nuclei. Adapted with permission from [15,65].

printing speed have great effects on the superficial structures of the polymerized soybean oil epoxidized acrylate (Fig. 8a). These scaffolds can fully recover their original shape at human body temperature (37 °C) from a temporary shape set at −18 °C. This novel material showed significantly higher hMSC adhesion and proliferation than polyethylene glycol diacrylate (PEGDA), and had no statistical difference from PLA and PCL. The growth of hMSCs on the printed scaffolds is shown in Fig. 8b. Given the multipotent nature of hMSCs, these printed scaffolds have great potential applications for osteochondral and neural tissue engineering. Graded, complex, porous structures were fabricated by using castor oil based polymers, as shown in Fig. 8c [65]. With PCL serving as a control, hMSC adhesion, proliferation, and differentiation greatly increased on these novel smart polymers, and the proliferation of hMSCs on different materials is demon-

strated in Fig. 8d [65]. The utilization of plant oil polymers will also advance the study of bio-based polymers for biomedical applications [56].

3D-printed objects that exhibit a designed shape change under tissue growth and resorption conditions over time were created with PCL to treat infants with severe tracheobronchomalacia [111]. The printed supporting structure had a customized design for patients less than 1 year old which accommodates changes in airway size by expanding as the patient ages over 3 years (Fig. 9a). The material also completely degraded after 3 years (Fig. 9b) when the matured airways were able to function unaided. In the study, the degradation and expansion of the printed PCL device concurred with the growth of the tracheo-bronchial tree over time, which is claimed as a 4D effect. This study implies the great application potential of 4D devices which
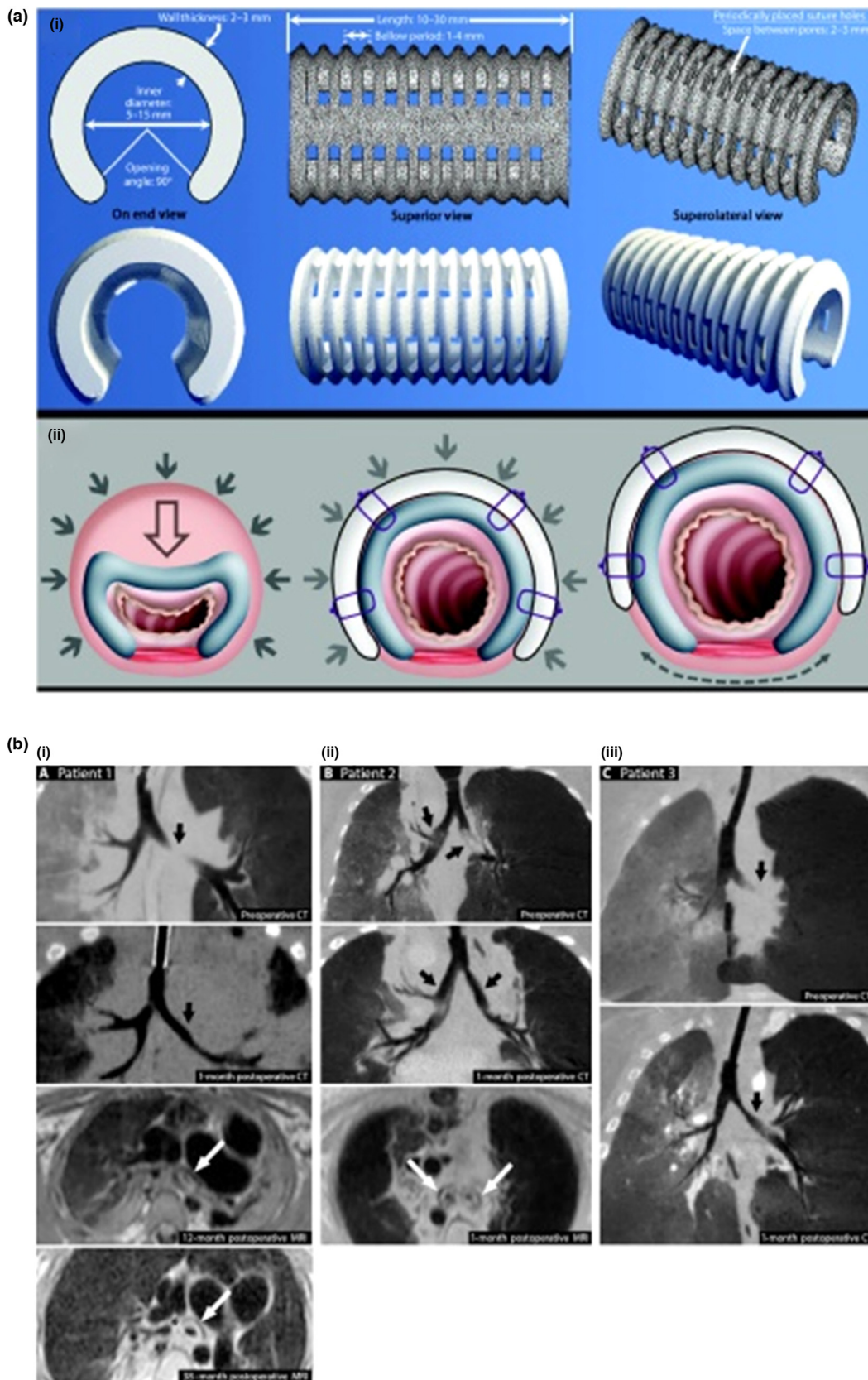
RESEARCH: Review

FIGURE 9

(a) Computational image-based design of 3D-printed tracheobronchial splints. (b) Pre- and post-operative imaging of patients. (i) Preoperative (top) and 1-month postoperative (upper middle) CT images of patient 1. Postoperative MRI (lower middle) demonstrated presence of splint around left bronchus in patient 1 at 12 months and focal fragmentation of splint due to degradation at 38 months (bottom). (ii) Preoperative (top) and 1-month postoperative (upper middle) CT images of patient 2. Postoperative MRI (lower middle) demonstrated presence of splints around the left and right bronchi in patient 2 at 1 month. (iii) Preoperative (top) and 1-month postoperative (bottom) CT images of patient 3. Adapted with permission from [111].

adapt to growing or changing tissues, particularly for pediatric applications.

Perspective and conclusions

Various 3D printing technologies have been utilized for 3D biofabrication, including STL, and FDM. Artificial tissues and organs can be fabricated directly with subsequent cell culturing and/or implantation; alternatively, biological constructs encapsulating cells and bioactive agents can be directly printed by using cell-containing inks [72]. Although the currently popular forms of 4D printing are polyjet printing and syringe printing, all other 3D printing platforms definitely have strong potential to contribute to the future of 4D printing.

In addition to structural design and printing techniques, ink materials are extremely crucial for achieving a 4D effect. The synthesis and development of 4D inks requires a high level of expertise and significant effort [112,113]. Specific to tissue and organ regeneration applications, the printing materials must be biocompatible and capable of performing dynamic 4D processes in a physiological environment. Unfortunately, most reported materials have been designed for non-biomedical applications, and exterior stimuli are extremely harsh for tissue and organ function. For a long period of time, the biomedical field has concentrated on the study of hydrogels which are also a material of focus for 4D printing [114,115]. Novel and multi-functional 4D inks are no doubt highly desirable for further expansion of 4D printing.

In summary, although 4D printing has shown great application potential and continues to generate attention, it is still in its infancy as a research area. In the future, 4D printing requires technological advances in various fields including software, modeling, mechanics and chemistry. Self-assembling materials have been intensively studied for decades, but only a small portion of these materials have been investigated for 4D printing. Multi-responsive structures triggered by various stimuli necessitate greater efforts and expertise. More importantly, the structures have to meet specific requirements for tissue and organ regeneration applications, such as biodegradability and biocompatibility properties. 4D printing may provide a novel platform for biomedical studies of functional synthetic tissues and organs. The advanced characteristics of 4D printing and the expected plethora of unexplored research areas project a fast developmental path with a wide application range of multiple dimensional printing, not only in the tissue and organ regeneration realm but throughout all areas of science and technology.

Acknowledgements

References

[1] S. Tibbits, TED talk, 2013. http://www.ted.com/talks/skylar_tibbits_the_emergence_of_4d_printing/transcript?language=en.
[2] A.S. Gladman et al., Nat. Mater. 15 (2016) 413.
[3] R.L. Truby et al., Nature 540 (7633) (2016) 371.
[4] S. Tibbits, http://www.sjet.us/MIT_4D%20PRINTING.html.
[5] S. Tibbits et al., ACADIA (2014) 539.
[6] S. Tibbits, Architect Des. 82 (2) (2012) 68.
[7] S.T. Thomas, A. Campbell, Banning Garrett The Atlantic Council of the United States, 2014.
[8] Q. Zhao et al., Prog. Polym. Sci. 49 (2015) 79.
[9] M.D. Hager et al., Prog. Polym. Sci. 49 (2015) 3.
[10] S. Miao et al., J. Am. Oil Chem. Soc 90 (9) (2013) 1415.
[11] S. Miao et al., Eur. J. Lipid Sci. Technol. 114 (12) (2012) 1345.
[12] Y. Zhou et al., J. Mech. Sci. Technol. 29 (10) (2015) 4281.
[13] E. Pei, Assemb. Autom. 34 (4) (2014) 310.
[14] L. Huang et al., Adv. Mater. 29 (2016) 1605390.
[15] S. Miao et al., Sci. Rep. 6 (2016) 27226.
[16] M. Zarek et al., Virt. Phys. Prototyp. 11 (4) (2016) 263.
[17] J. Choi et al., 3D Print. 2 (4) (2015) 159.
[18] S. Bose et al., Mater. Today 16 (12) (2013) 496.
[19] S.A. Khaled et al., Int. J. Pharm. 461 (1) (2014) 105.
[20] J. Zhang et al., Int. J. Pharm. 519 (2016) 186.
[21] Z.-Z. Zhang et al., Acta Biomater. 43 (2016).
[22] X. Li et al., Regenerative biomaterials, 2015.
[23] Z.-Z. Zhang et al., RSC Adv. 5 (95) (2015).
[24] H.l. Thérien-Aubin et al., J. Am. Chem. Soc. 135 (12) (2013) 4834.
[25] B. Gao et al., Trends Biotechnol. 34 (9) (2016) 746.
[26] Y.-C. Li et al., Biofabrication 9 (1) (2016) 012001.
[27] F. Momeni et al., Mater. Des. 122 (2017) 42.
[28] Y. Liu et al., Soft Matter 8 (6) (2012) 1764.
[29] G. Villar et al., Science 340 (6128) (2013) 48.
[30] S. Tibbits, Architect Des. 84 (1) (2014) 116.
[31] D. Raviv et al., Sci. Rep. 4 (2014) 7422.
[32] D. Correa et al., 3D Print. 2 (3) (2015) 106.
[33] J. Girdis et al., JOM 69 (3) (2016) 575.
[34] A. Le Duigou et al., Mater. Des. 96 (2016) 106.
[35] Y. Mao et al., Sci. Rep. 6 (2016) 24761.
[36] D. Kokkinis et al., Nat. Commun. 6 (2015) 8643.
[37] B.G. Compton et al., Adv. Mater. 26 (34) (2014) 5930.
[38] J.J. Martin et al., Nat. Commun. 6 (2015) 8641.
[39] Q. Ge et al., Appl. Phys. Lett. 103 (13) (2013) 131901.
[40] Q. Ge et al., Smart Mater. Struct. 23 (9) (2014) 094007.
[41] Q. Ge et al., Sci. Rep. 6 (2016) 31110.
[42] H. Meng et al., Polymer 54 (9) (2013) 2199.
[43] Y. Liu et al., Smart Mater. Struct. 23 (2) (2014) 023001.
[44] Q. Zhao et al., Sci. Adv. 2 (1) (2016) e1501297.
[45] A. Lendlein et al., Angew. Chem. Int. Ed. 41 (12) (2002) 2034.
[46] A. Lendlein et al., Adv. Mater. 22 (31) (2010) 3344.
[47] L. Fang et al., Macromol. Mater. Eng. 301 (1) (2016) 1111.
[48] L. Fang et al., Compos. Sci. Technol. 138 (2017) 106.
[49] M. Zarek et al., Adv. Mater. 28 (2015) 4449.
[50] H. Wei et al., ACS Appl. Mater. Interfaces 9 (1) (2016) 876.
[51] M. Zarek et al., Macromol. Rapid Commun. 38 (2) (2016) 1600628.
[52] N.J. Castro et al., Nanoscale 7 (33) (2015) 14010.
[53] Y. Mao et al., Sci. Rep. 5 (2015) 13616.
[54] M. Bodaghi et al., Smart Mater. Struct. 25 (10) (2016) 105034.
[55] J. Wu et al., Sci. Rep. 6 (2016) 24224.
[56] S. Miao et al., Acta Biomater. 10 (4) (2014) 1692.
[57] J.-M. Raquez et al., Prog. Polym. Sci. 35 (4) (2010) 487.
[58] V.K. Thakur et al., Carbohydr. Polym. 109 (2014) 102.
[59] M. Galià et al., Eur. J. Lipid Sci. Technol. 112 (1) (2010) 87.
[60] S. Miao et al., J. Polym. Sci. A: Polym. Chem. 48 (1) (2010) 243.
[61] S. Miao et al., J. Appl. Polym. Sci. 127 (3) (2013) 1929.
[62] S. Miao et al., Eur. J. Lipid Sci. Technol. 114 (10) (2012) 1165.
[63] S. Miao et al., J. Polym. Sci. A: Polym. Chem. 46 (12) (2008) 4243.
[64] S. Miao et al., Eur. J. Lipid Sci. Technol. 117 (2) (2015) 156.
[65] S. Miao et al., Tissue Eng. C: Methods 22 (10) (2016) 952.
[66] N.J. Castro et al., Cell Mol. Bioeng. 8 (3) (2015) 416.
[67] B. Holmes et al., Nanotechnology 27 (6) (2016) 064001.
[68] H. Cui et al., Adv. Healthc. Mater. 5 (17) (2016) 2174.
[69] H. Cui et al., Adv. Sci. 3 (2016) 1600058.
[70] S.-J. Lee et al., Neural Engineering, Springer, 2016, pp. 1–24.
[71] T. Guo et al., Tissue Eng. B: Rev. (2016), https://doi.org/10.1089/ten.teb.2016.03161.
[72] H. Cui et al., Adv. Healthc. Mater. 6 (2016) 1601118.
[73] M.A. Nowicki et al., Nanotechnology 27 (41) (2016) 414001.
[74] Y. Yang et al., Int. J. Adv. Manuf. Technol. 84 (9–12) (2016) 2079.

[75] SMP Technologies, Homepage for Product Information, 2009. http://www2.smptechno.com/en/smp/.
[76] F. Senatov et al., J. Mech. Behav. Biomed. 57 (2016) 139.
[77] A.B. Kutikov et al., Macromol. Chem. Phys. 215 (24) (2014) 2482.
[78] X. Gu et al., Polymer 53 (25) (2012) 5924.
[79] S. Shaffer et al., Polymer 55 (23) (2014) 5969.
[80] Q. Zhang et al., Sci. Rep. 5 (2015) 8936.
[81] Q. Zhang et al., Sci. Rep. 6 (2016) 22431.
[82] C. Li et al., Soft Matter 7 (16) (2011) 7511.
[83] Y. Hu et al., Adv. Mater. 27 (47) (2015) 7867.
[84] J. Mu et al., Sci. Adv. 1 (10) (2015) e1500533.
[85] X. Mu et al., Soft Matter 11 (13) (2015) 2673.
[86] D.L. Taylor, Adv. Mater. 28 (41) (2016) 9060.
[87] S. Hou et al., Adv. Healthc. Mater. 4 (10) (2015) 1491.
[88] D.M. Kirchmajer et al., J. Mater. Chem. B 3 (20) (2015) 4105.
[89] C.J. Ferris et al., Soft Matter 9 (14) (2013).
[90] E. Caló et al., Eur. Polym. J. 65 (2015) 252.
[91] E.A. Appel et al., Nat. Commun. 6 (1–9) (2015).
[92] L. Li et al., Adv. Mater. 27 (7) (2015) 1294.
[93] S.E. Bakarich et al., ACS Appl. Mater. Interfaces 6 (18) (2014) 15998.
[94] O. Kuksenok et al., Mater. Horiz. 3 (1) (2016) 53.
[95] K. Kuribayashi-Shigetomi et al., PLoS ONE 7 (12) (2012) e51085.
[96] V. Maruthamuthu et al., Proc. Natl. Acad. Sci. U. S. A. 108 (12) (2011) 4708.
[97] P.K. Kundu et al., Nat. Chem. 7 (8) (2015) 646.
[98] S.V. Murphy et al., Nat. Biotechnol. 32 (8) (2014) 773.
[99] S.-J. Lee et al., Tissue Eng. (2016), https://doi.org/10.1089/ten.tea.2016.0353(ja).
[100] X. Zhou et al., ACS Appl. Mater. Interfaces 8 (44) (2016) 30017.
[101] W. Zhu et al., Nanotechnology 27 (31) (2016) 315103.
[102] S.-J. Lee et al., IEEE Trans. Biomed. Eng. 64 (2) (2016) 408.
[103] W. Zhu et al., Nanomed. Nanotech. Biol. Med. 12 (1) (2016) 69.
[104] W. Zhu et al., Acta Biomater. 14 (2015) 164.
[105] B. Holmes et al., Tissue Eng. A 21 (1–2) (2014) 403.
[106] C.M. O'Brien et al., Tissue Eng. B Rev. 21 (1) (2014) 103.
[107] W. Zhu et al., Nanomedicine 9 (6) (2014) 859.
[108] M.J. Booth et al., Biochem. Biochem. Soc. 38 (4) (2016) 16.
[109] G. Villar et al., Nat. Nanotechnol. 6 (12) (2011) 803.
[110] M.J. Booth et al., Sci. Adv. 2 (4) (2016) e1600056.
[111] R.J. Morrison et al., Sci. Transl. Med. 7 (285) (2015) 285ra64.
[112] D. Chimene et al., Ann. Biomed. Eng. 44 (6) (2016) 2090.
[113] T. Jungst et al., Chem. Rev. 116 (3) (2015) 1496.
[114] S. Naficy et al., Macromol. Mater. Eng. 302 (2016) 1600212.
[115] S.E. Bakarich et al., Macromol. Rapid Commun. 36 (12) (2015) 1211.